

THE IONIZATION STATE OF SODIUM IN GALACTIC WINDS

NORMAN MURRAY^{1,2}, CRYSTAL L. MARTIN^{3,4,5}, ELIOT QUATAERT^{3,4,6}, & TODD A. THOMPSON^{7,8}*Draft version October 31, 2018*

ABSTRACT

Roughly 80% of Ultraluminous Infrared Galaxies (ULIRGs) show blue shifted absorption in the resonance lines of neutral sodium, indicating that cool winds are common in such objects, as shown by Rupke et al and by Martin. The neutral sodium (NaI) columns indicated by these absorption lines are $\sim 10^{13} - 3 \times 10^{14} \text{ cm}^{-2}$, while the bolometric luminosity varies by a factor of only four. We show that the gas in ULIRG outflows is likely to be in photoionization equilibrium. The very small ULIRG sample of Goldader et al. demonstrates that the ratio of ultraviolet flux to far infrared flux varies by a factor ~ 100 from object to object. While the Goldader sample does not overlap with those of Rupke et al. and Martin, we show that such a large variation in ultraviolet flux will produce a similar variation in the column of neutral sodium for a fixed mass flux and density. However, if the cold gas is in pressure equilibrium with a hot outflow with a mass loss rate similar to the star formation rate, the range of ionization state is significantly smaller. Measurements of the UV flux for objects in the Martin and Rupke et al. catalogs will definitively determine if photoionization effects are responsible for the wide variation seen in the sodium columns. If they are, a determination of the gas density and mass loss rate in the cool winds will follow, with attendant improvements in our understanding of wind driving mechanisms and of the effects of galaxies on their surroundings.

Subject headings: galaxies:general — galaxies:formation — galaxies:intergalactic matter — galaxies:starburst — galaxies:fundamental parameters

1. INTRODUCTION

Recent observations of the sodium resonance line (NaD) doublet in Ultra-luminous Infra-red Galaxies (ULIRGS) by Rupke and coworkers Rupke et al. (2002), Rupke & Veilleux (2005), Rupke et al. (2005a), Rupke et al. (2005b) and by Martin (2005; 2006) show that cool outflows from ULIRGS are common. Martin (2005) finds that 15 of 18 ULIRGS (83%) possess such flows, while Rupke et al. (2005b) find a detection rate of $80 \pm 7\%$ for 30 local ULIRGs. These results indicate that the outflow emerges in most directions. The absorption troughs, which typically extend over $\sim 300 \text{ km s}^{-1}$, are not black, which at first blush might suggest that the outflows are optically thin in the NaD line. However, the doublet line ratio, which is equal to 2:1 in optically thin gas, rarely has that ratio in Martin's sample, while Rupke et al. (2005a) find optical depths for the weaker of the doublet lines that range from 0.06 to 7, with an average of 1.5. This finding shows that some sight lines to ULIRG galaxies are optically thick in the NaD line, that the optically thick outflow covers only about 25–30% of the (optically emitting)

galaxy, but that this optically thick component is seen toward $\sim 80\%$ of ULIRGS. Given the patchy nature of the interstellar medium in most galaxies, the last finding is not entirely surprising.

However, another implication of the observations is very surprising. As Figure 1 shows, the mean column averaged over both samples (Rupke et al. 2005a; Martin 2006) is 13.7 in the log, with a standard deviation of 0.66 dex, or from 10^{13} cm^{-2} to $3 \times 10^{14} \text{ cm}^{-2}$. The actual Na I columns vary from $7 \times 10^{12} \text{ cm}^{-2}$ to $5 \times 10^{14} \text{ cm}^{-2}$ in the sample of Rupke et al. (2005a). Since the luminosity, and star formation rate of the galaxies in both samples varies by only a factor of about 4 (the standard deviation is a factor of 2), one might expect the N_H column and hence the N_{NaI} column toward the galaxies to vary by a similar factor; in simple galactic wind models the mass outflow rate increases with increasing star formation rate.

The Na I column can be used to find the mass loss rate from each galaxy, in principle. For example, in a smooth flow, the density is related to the mass loss rate by

$$\dot{M}_w = \Omega r^2 \mu(r) n(r) v(r), \quad (1)$$

¹Canada Research Chair in Astrophysics²Canadian Institute for Theoretical Astrophysics, 60 St. George Street, University of Toronto, Toronto, ON M5S 3H8, Canada; murray@cita.utoronto.ca³Packard Fellow⁴Alfred P. Sloan Research Fellow⁵University of California, Santa Barbara, Department of Physics, Santa Barbara, CA 93106; cmartin@physics.ucsb.edu⁶Astronomy Department & Theoretical Astrophysics Center, 601 Campbell Hall, The University of California, Berkeley, CA 94720; eliot@astro.berkeley.edu⁷Princeton University Observatory, Peyton Hall, Princeton NJ 08544-1001; thomp@astro.princeton.edu⁸Lyman Spitzer Jr. Fellow

where $\mu(r)$ is the mean molecular weight, $n(r)$ is the number density of hydrogen, $v(r)$ is the velocity of the flow at a distance r from the center of the galaxy, and $\Omega \leq 4\pi$ is the global wind cover factor in steradians. For simplicity we employ a spherical model, although ULIRGs appear to form a substantial fraction of their stars in a kiloparsec (or smaller) scale disk Condon et al. (1991).

The hydrogen column through such a wind is

$$N_H = \frac{\dot{M}_w}{\Omega} \int_{r_0}^{\infty} \frac{dr}{r^2 \mu(r) v(r)}. \quad (2)$$

A very rough estimate is found by taking $\mu(r) = m_p$ and $v(r) = v_\infty$, where the latter is the terminal velocity of the outflow, which in the spirit of approximation adopted here is taken to be the maximum observed blue shift:

$$N_H \approx \frac{\dot{M}_w}{\Omega m_p v_\infty r_0}, \quad (3)$$

where r_0 is the radius at which the absorption line forms. Solving for the mass loss rate in terms (as far as possible) of observed quantities,

$$\dot{M}_w \approx \Omega m_p r_0 v_\infty N_{NaI} \left(\frac{N_{Na}}{N_{NaI}} \right) \left(\frac{N_H}{N_{Na}} \right) d_{Na}, \quad (4)$$

where N_{NaI} is the (observed) column of gas phase neutral sodium, N_{Na} the total gas phase sodium column, N_H is the total hydrogen column, and d_{Na} is the ratio of total to gas phase Na; it is larger than unity since much of the Na is locked up in dust grains. Neither of the two terms in parentheses nor d_{Na} are measured, nor is r_0 well constrained. For solar abundances $N_H/N_{Na} = 4.9 \times 10^5$ Anders & Grevesse (1989), while Savage & Sembach (1996) find that the gas phase abundance of Na in the cool gas of the diffuse cloud toward ζ Ophiuci is a factor of $d_{Na} = 8.9$ smaller than the solar abundance of Na. There is evidence of dust in ULIRG outflows; first, NaD is a resonance line, so that it scatters continuum photons rather than destroying them. Since the winds are nearly spherical (they are seen toward 80% of ULIRGS), any photons removed from our line of sight by the NaD transition should appear along some other line of sight as redshifted emission; since we see no such emission, some other mechanism is removing the scattered photons, absorption by dust being the number one suspect. Second, there is a correlation seen between reddening and NaD absorption toward luminous infrared galaxies, again suggesting dust in the outflow Veilleux et al. (1995); Heckman et al. (2000). In the rest of this paper we will adopt solar metallicities and the Milky Way ISM d_{Na} just quoted. Using these values, the typical observed column $NaI = 10^{14} \text{ cm}^{-2}$ would correspond to a hydrogen column $N_H \approx 10^{21} \text{ cm}^{-2}$ if somewhat less than half the gas-phase sodium were neutral.

Any local heating, such as might be produced by shocks, will lead to lower depletion levels, but by less than the factor of ten corresponding to all the grains being destroyed, given the evidence for dust cited above.

The force responsible for expelling the wind is uncertain. One candidate is ram pressure from outflowing supernova-heated gas, which will entrain cold gas from the interstellar

medium of the ULIRG. A variant on this is ram pressure from hot gas produced by an accreting massive black hole (an active galactic nucleus, or AGN). The Compton temperature of both Seyfert and Quasar nuclei is around 10^7 K , similar to that from supernova heating. Momentum driving from supernovae can be significant, if most supernovae explode while surrounded by cold gas. Another candidate for momentum driving is radiation pressure on dust grains embedded in the cold gas. The radiation could arise either from stars or from a central black hole. The radiation pressure from a black hole can exceed that from a starburst. Whether such a centrally driven outflow can produce an outflow that will be detected from 80% of the sky is far from certain.

In fact it seems likely that both energy and momentum driving operate. ULIRGS are enveloped in x-ray emitting gas, Arp 220 being an excellent example McDowell et al. (2003), Clements et al. (2002); the presence of hot gas is a necessary (but not sufficient) condition for energy driving of a cool outflow. As we have just noted, the winds are most likely dusty. The wind optical depth to optical or UV emission is likely substantial, while the galaxies themselves are optically thick even to the far infrared. The outflow may well be multiphase; the questions to be addressed revolve around which phase carries more mass, momentum, energy, and metals into the surrounding intergalactic medium.

To answer such questions, we would like to measure the mass loss rate in cold gas. If the NaI columns are taken at face value, and the ratio N_H/N_{NaI} is assumed to be constant, the mass loss rates in cold gas vary from ULIRG to ULIRG by a factor of ~ 50 . Is this really true?

There are numerous possible reasons for the NaI column seen in galactic outflows to vary from object to object. The mass loss rate will vary from object to object, so that the total column of hydrogen, and hence Na, will vary, even at a fixed metallicity. The metallicity of the outflowing gas may vary from object to object. Both these properties are likely to depend on the star formation rate (and history); the star formation rate, at least, varies over only a small range for the samples we are discussing. A more likely cause of variation in NaI column is a variation in either or both the depletion on to dust grains and the ionization state of Na. Neutral sodium is a rather delicate atom, easily ionized by ultraviolet radiation. The wind may be irradiated either by starlight from the host galaxy, or by shocks in the wind.

In this paper we argue that the outflow is in photoionization equilibrium, except possibly for the most UV dim systems, and then show that if Martin and Rupke et al.'s galaxies have spectral energy distributions like those of other nearby ULIRGs that have been observed in the ultraviolet, then it may be that the mass loss rates are more nearly equal than the observed NaD columns imply; unless the neutral gas is very dense, $n \sim 10^5 \text{ cm}^{-3}$, the ionization fraction, or the ratio of neutral to total sodium, (NaI/Na), will vary by a large factor from object to object. This follows from the observed variation of ~ 100 in the ratio of UV to FIR flux seen in nearby ULIRGs (Goldader et al. 2002), and simple photoionization calculations, as we show below.

2. NEUTRAL SODIUM GAS ABUNDANCES

The ionization state of the wind depends on the gas density, the ionizing flux, and the gas temperature. We start by estimating the gas density. We will use canonical values for the luminosity $L_{FIR} = 10^{12}L_{\odot}$ and terminal wind velocity $v_{\infty} = 300 \text{ km s}^{-1}$.

To obtain a rough lower limit for the density we will assume a smooth dust driven wind, which captures the entire momentum output of the galaxy along a particular sight line. Following Rupke et al. (2005b) we let C_{Ω} denote the fraction of sight lines that pass through a wind and C_f denote the local cover factor of NaI gas (along a sight line through the wind), so that $\Omega/4\pi = C_{\Omega}C_f$. Rupke et al. (2005b) find $C_{\Omega} = 0.8$ as noted above, and $C_f \approx 0.4$ (their table 2) for local ULIRGs, values which we will adopt. In that case the mass loss rate is given by

$$\dot{M}_w = \frac{L_{FIR}}{cv_{\infty}} C_{\Omega} C_f. \quad (5)$$

For our canonical numbers, this yields a mass loss rate of $\dot{M}_w \approx 22M_{\odot} \text{ yr}^{-1}$. The star formation rate needed to power the bolometric luminosity ($10^{12}L_{\odot}$) is $\dot{M}_* = L/(\epsilon c^2) \approx 90M_{\odot} \text{ yr}^{-1}$, where $\epsilon \approx 8 \times 10^{-4}$ for a Salpeter IMF with stellar masses between 0.1 and $100M_{\odot}$. The ratio η of mass outflow rate to star formation rate is

$$\begin{aligned} \frac{\dot{M}_w}{\dot{M}_*} &= C_{\Omega} C_f \epsilon \frac{c}{v_{\infty}} \\ &\approx 0.256 \left(\frac{C_{\Omega}}{0.8} \right) \left(\frac{C_f}{0.4} \right) \left(\frac{\epsilon}{8 \times 10^{-4}} \right) \left(\frac{300 \text{ km s}^{-1}}{v_{\infty}} \right) \end{aligned} \quad (6)$$

Rupke et al. (2005b), using a sample of 30 low redshift ULIRGs, find $\eta = 0.19_{-0.1}^{+0.5}$; the error bars do not include the large uncertainty in the NaI/Na ratio.

Estimates of mass loss rates in supernova driven winds also tend to yield results comparable to the star formation rate, e.g., Martin (1999), although it is unclear if the hot gas actually escapes from the galaxy in massive galaxies.

Combining equations (1) and (5) yields the estimated density

$$n(r, v; L_{FIR}) = \frac{L_{FIR}}{4\pi\mu v_{\infty} cr^2 v(r)}. \quad (7)$$

Using the canonical values quoted above, $\mu = 1.38m_p$, and $r = 500 \text{ pc}$, we find

$$n \approx 6 \left(\frac{L}{10^{12}L_{\odot}} \right) \left(\frac{300 \text{ km/s}}{v_{\infty}} \right) \left(\frac{100 \text{ km/s}}{v} \right) \left(\frac{500 \text{ pc}}{r} \right)^2 \text{ cm}^{-3}, \quad (8)$$

We have chosen $r = 500 \text{ pc}$ since this is (roughly) the size of both CO ($\sim 500 \text{ pc}$, Solomon et al. 1997) and radio disks ($\sim 100 \text{ pc}$, Condon et al 1991) in typical ULIRGs. The distance between the disk and the outermost point of the outflow will depend on age, and is likely to be much larger than 500 pc , but most of the column will be accumulated at small radii, see equation (3). While we have derived this result for a smooth cool outflow, a hot supernova driven outflow with the same mass loss rate will have the same density, as can be seen from equation (1).

If the gas is clumpy, the relevant density will be higher than this estimate, for the same mass loss rate. In particular, if the cool gas is driven out of the galaxy by ram pressure from a hot outflow, the cool gas should be in or near pressure balance with the hot wind. In that case,

$$n \approx n_h \frac{T_h}{T}, \quad (9)$$

where the subscript h denotes supernova heated gas. The hot gas has $T_h \approx 10^7 \text{ K}$, while the cold gas has $T \lesssim 100$, as shown by the numerical results described below. If the mass loss rate in hot gas is of order the star formation rate, the cold gas has $n \gtrsim 6 \times 10^5 \text{ cm}^{-3}$ near the launching radius. This is slightly higher than the density of the ISM in the inner disks of ULIRGs. Since the ionization state of the gas depends on the gas density, it may be possible to distinguish between ram pressure driven flows and dust driven flows. We will return to this point in §4.

2.1. Timescales

With this estimate of the gas density we are in a position to estimate several relevant time scales. The first is the dynamical time scale,

$$\tau_{\text{dyn}} \approx 5 \times 10^{13} \left(\frac{r}{500 \text{ pc}} \right) \left(\frac{300 \text{ km s}^{-1}}{v_{\infty}} \right) \text{ s}. \quad (10)$$

In a clumpy flow, the size of the cold clumps should be much less than the size of the galaxy. For example, in our own galaxy, observations of cool gas on top of the hot outflow GSH 242-03+37 (McClure-Griffiths et al. 2005) indicate that the cool gas has a length scale l of order tens of parsecs, while sitting on hot gas 1,500 parsecs above the galactic plane. The sound crossing time for such clumps is

$$\tau_{h, MW} \approx 10^{12} \left(\frac{l}{10 \text{ pc}} \right) \left(\frac{300 \text{ km s}^{-1}}{c_h} \right) \text{ s} \quad (11)$$

for the surrounding hot gas. These clumps have a column density $N_H \approx 3 \times 10^{19} \text{ cm}^{-2}$, a factor of about ten lower than the column through the disk of the Milky Way, and a density $n = N_H/l \sim 1 \text{ cm}^{-3}$ for the observed size $l = 10 \text{ pc}$, a density similar to that in the disk as a whole.

In order to estimate the time scale for the evolution of the cold outflowing gas in ULIRGs, we need to estimate the length scale of the cold gas. To estimate the size of a clump of cold gas driven out of a ULIRG disk by a hot outflow, we use the inferred N_H for the NaI carrying outflow, and assume that the initial gas density is equal to that in the disk midplane, as is the case in the Milky Way; $l = N_H/n = 10^{21} \text{ cm}^{-2}/10^5 \text{ cm}^{-3} = 10^{16} \text{ cm}$. In Arp 220, the star forming disk(s) have $r \approx 100 \text{ pc}$ with a disk scale height H satisfying $H/r \approx 0.1$ Sakamoto et al. (1999), so $l/H \approx 3 \times 10^{-3}$, a factor of ten or so smaller than ratio of 0.05 seen in the Milky Way.

This short length scale has important implications for the pressure and hence the density in the NaI bearing gas. To work out these implications, we first show that if the hot gas is responsible for pushing the cold gas out of the

galaxy, the mass loss rate in the hot gas must exceed that of the cold gas by the factor $4\pi/\Omega \approx 5$. We then show that the density of the cold gas is $n \gtrsim 6 \times 10^5 \text{ cm}^{-3}$ for our canonical numbers. Gas of this density exposed to the radiation from a ULIRG will be neutral, with all the gas-phase Na in the form of NaI.

We assume that the cool gas seen in ULIRG outflows comes in roughly spherical clumps of radius l , with column $N_H \approx 10^{21} \text{ cm}^{-2}$. These clumps are pushed out of the galaxy by ram pressure from the hot outflow, which exerts a force Murray et al. (2005)

$$F_{ram} = m_p n_h v_h^2 \pi l^2, \quad (12)$$

where v_h is the velocity of the hot outflow. This force must exceed the force of gravity,

$$F_{grav} = \frac{v_c^2}{r} m_p n, \quad (13)$$

where v_c is the circular velocity of the galactic disk; we note that $v_c \lesssim v_h$. Introducing the cover factor Ω_h of the hot gas (which should be close to 4π since the sound speed of the hot gas is comparable to the bulk velocity of the gas), we find that the mass loss rate of the hot gas must exceed

$$\dot{M}_h \gtrsim \left(\frac{\Omega_h}{\Omega}\right) \left(\frac{v_c}{v}\right) \left(\frac{v_c}{v_h}\right) \dot{M}_w \quad (14)$$

if the hot gas is to accelerate the cold clouds out of the galactic potential.

The mass loss rate in hot gas must exceed that in cold gas by the ratio of the cover factors; we expect that this is roughly the inverse of $C_f C_\Omega$, or about a factor of five. For ram pressure driving to be important, the density of the hot gas should be that given by eqn. (8).

The hot gas will travel across any embedded cold clump in a time

$$\tau_h \approx 3 \times 10^8 \left(\frac{l}{10^{16} \text{ cm}}\right) \left(\frac{300 \text{ km s}^{-1}}{c_h}\right) \text{ s}, \quad (15)$$

much shorter than the dynamical time.

In a supernova driven flow shocks may be driven into the cold clouds. Let us suppose that the mass loss rate in hot gas is equal to the star formation rate (and thus a factor ~ 5 times the observed mass loss rate of the cold gas in ULIRGs). The pressure in the cold clouds is

$$P_c = 1.38 \times 10^{-9} \left(\frac{n}{10^5 \text{ cm}^{-3}}\right) \left(\frac{T}{100 \text{ K}}\right) \text{ dynes cm}^{-2}, \quad (16)$$

while the pressure in the hot gas is

$$P_h \approx 8 \times 10^{-9} \left(\frac{n_h}{6 \text{ cm}^{-3}}\right) \left(\frac{T}{10^7 \text{ K}}\right) \text{ dynes cm}^{-2}, \quad (17)$$

This over-pressured (from the point of view of the cold gas) hot gas moves at its sound speed, which is a factor of 100 or more higher than the thermal sound speed in the cold gas. A cold gas cloud that is exposed to the hot gas

will experience a six-fold increase in external pressure in a time of order one percent of the cloud dynamical time, i.e., it sees what is effectively an instantaneous jump in its external pressure. The result will be a shock of Mach number $\sim \sqrt{6}$ propagating into the cloud. If the initial density of the cold gas is smaller, the shock will be stronger.

These shocks will cross the cloud in a time

$$\tau_s \approx 5 \times 10^{10} \left(\frac{l}{10^{16} \text{ cm}}\right) \left(\frac{v_s}{2 \text{ km s}^{-1}}\right), \quad (18)$$

where $v_s = \sqrt{P_h/m_p n}$ is the shock velocity. Since this is much less than the outflow time given by equation (10), the cold clumps should be in pressure equilibrium with the hot gas, if the hot gas is dynamically important; this statement is true even for l a factor of 10 or 100 larger than our fiducial value of 10^{16} cm . Indeed, in our galaxy, McClure-Griffiths et al. (2005) conclude that the clumps they see are in pressure equilibrium with the surrounding hot gas.

We have assumed that the shock is isothermal. In fact, the cooling time for the postshock gas is:

$$\tau_{cool} \approx 1.5 \times 10^7 \left(\frac{T_s}{10^3 \text{ K}}\right) \left(\frac{3 \times 10^{-26} \text{ erg}^{-1} \text{ cm}^3 \text{ s}^{-1}}{\Lambda}\right) \left(\frac{3 \times 10^5 \text{ cm}^{-3}}{n_s}\right) \text{ s}, \quad (19)$$

where we have scaled to a post-shock temperature T_s appropriate for a 2 km s^{-1} shock. The numerical value for Λ is from Dalgarno & McCray (1972). The cooling length $\tau_{cool} v_s \approx 4 \times 10^{12} \text{ cm}$, much shorter than any other length in the problem, so the shock is effectively isothermal. The cooling column, $\tau_{cool} v_s n \approx 10^{18} \text{ cm}^{-3}$, consistent with the general result given by McKee & Hollenbach (1980). In fact this result is more general. Any shock propagating through dense gas will cool on a time scale short compared to the outflow time at $r = 500 \text{ pc}$. The maximum cooling column is McKee & Hollenbach (1980)

$$N_{cool} \approx 10^{19} - 10^{20} \text{ cm}^{-3}, \quad (20)$$

for $v_s < 20 \text{ km s}^{-1}$, and less for higher shock velocities.

The minimum value for $\Lambda \approx 10^{-26} \text{ erg}^{-1} \text{ cm}^3 \text{ s}^{-1}$ Dalgarno & McCray (1972) for $T \gtrsim 30 \text{ K}$, so as long as $n > 10 \text{ cm}^{-3}$ the gas will cool to 30 K in less than the outflow time.

This result shows that, in the event that the initially cool, dense component of the ISM is shocked and hence heated in the wind, it will quickly cool again. Since the ratio of temperatures of the hot and cold gas exceeds 10^5 , while, as we have just shown, the two are in pressure equilibrium, the density of the cold gas must exceed $n = 6 \times 10^5 \text{ cm}^{-3}$, as we stated above.

If the mass-loss rate in hot gas is less than the star formation rate, so that some mechanism other than ram pressure is responsible for expelling the cold gas from the galaxy, P_h will be similar to or smaller than the pressure in the cold clouds; the only shocks present will be those driven into the clouds by the ram pressure of the hot gas

as it encounters cold gas. The cold gas will not be pressure confined by the hot gas, so the cold gas will expand at its sound speed as it flows out. If the initial length scale is 10^{16} cm, and the mass loss rate is that given in equation (6), the cold gas will expand to a cover factor C_f of order unity by the time it is 500 pc from its launching radius.

The sodium ions in the post-shock gas will also quickly recombine once the gas cools, as we show next. The recombination time for sodium in cool $T \sim 100\text{K} - 1000\text{K}$ gas is

$$\tau_{rec} = \frac{1}{\alpha_{Na} n_e} \approx 10^{12} \left(\frac{0.06 \text{ cm}^{-3}}{n_e} \right) \text{ s.} \quad (21)$$

In this expression, α_{Na} is the total recombination coefficient of NaII to NaI. The radiative recombination coefficient $\alpha_{Na}(T = 100\text{K}) \approx 10^{-11} \text{ cm}^3 \text{ s}^{-1}$ Verner & Ferland (1996), which we have assumed dominates the recombination. We have scaled to the minimum electron density, for gas of any density, found in our numerical photoionization calculations using CLOUDY, described below. This minimum electron density occurs in gas with low density ($n = 6 \text{ cm}^{-3}$ and low UV/FIR flux ratios, $\sim 10^{-9}$; the electron density for SEDs with higher UV/FIR flux density ratios is much larger, leading to shorter recombination times.

For warm ionized gas, $T \approx 10^4\text{K}$, $n_e \approx n$, while $\alpha(T = 10^4) \approx 2 \times 10^{-13} \text{ cm}^3 \text{ s}^{-1}$. Thus, for any temperature between 100K and 10^4K the recombination time is far shorter than the dynamical time. We conclude that shocks are not an efficient mechanism for maintaining sodium atoms in a singly ionized state

As the gas flows away from the disk plane the density and pressure in the hot component will decrease as $1/r^2$, so the density in pressure confined cold clumps will also decrease, lengthening τ_{cool} . However the cooling time will remain short compared to the outflow time, which increases as r , out to megaparsec distances.

Even for a smooth flow not in pressure equilibrium with a massive hot outflow, the density $n \approx 6$, so the cooling time is $\tau_{cool} \approx 8 \times 10^{12}$ s, still short compared to the outflow time. However, if shocks occur at large enough distances, the cooling time may exceed the outflow time. Nominally this would occur at distances of order 5 kpc, but this neglects the compression of the gas in the shock.

The photoionization time is

$$\begin{aligned} \tau_{ion} &= \frac{4\pi r^2 \langle h\nu \rangle}{a_{NaI} L_{UV}} \\ &\approx 10^5 \left(\frac{r}{500 \text{ pc}} \right)^2 \left(\frac{10^{12} L_{\odot}}{L_{FIR}} \right) \left(\frac{L_{\nu}^{FIR}}{L_{\nu}^{UV}} \right) \text{ s,} \end{aligned} \quad (22)$$

where $a_{NaI} \approx 10^{-19} \text{ cm}^2$ Verner et al. (1996) is the photoionization cross section and $L_{UV} \approx \nu L_{\nu}^{UV}$ is the luminosity at the sodium edge. The photoionization time ranges between $\approx 10^9$ and 3×10^{11} s for observed UV/FIR flux density ratios (see Figure 2 for the flux density ratios).

We have seen that both the recombination time and the photoionization time are shorter than the dynamical time, at least for temperatures below 10^5K , while the post-shock

cooling time is shorter still. We conclude that the NaI laden gas is in photoionization equilibrium.

2.2. Photoionization equilibrium

Consider a dilute gas of number density n irradiated by the light from a ULIRG. We saw above that both the photoionization and recombination time scales are shorter than the dynamical time scale, so the ionization state of sodium is controlled by the flux near 5.139 eV, the ionization potential of Sodium I, and by the flux near the Lyman edge at 13.6 eV.

The Lyman edge flux controls whether the gas as a whole is neutral. In highly ionized gas, the neutral fraction of hydrogen is given by Osterbrock (1989)

$$\frac{n_0}{n} = \frac{\alpha_H}{a_H c} U^{-1} \approx 10^{-6} U^{-1}, \quad (23)$$

where $\alpha_H \approx 10^{-13} \text{ cm}^3 \text{ s}^{-1}$ is the recombination coefficient for hydrogen, $a_H \approx 6 \times 10^{-18} \text{ cm}^2$ is the photoionization cross section, c is the speed of light, and

$$U \equiv \frac{L_0 / \langle h\nu_0 \rangle}{4\pi r^2 n_e c} \quad (24)$$

is known as the ionization parameter. The rate of emission of ionizing photons, $L_0 / \langle h\nu \rangle$ is defined by

$$\frac{a_{\nu_0} L_0}{\langle h\nu_0 \rangle} \equiv \int_{\nu_0}^{\infty} d\nu \frac{a_{\nu} L_{\nu}}{h\nu}, \quad (25)$$

where ν_0 is the frequency at the Lyman edge, and L_{ν} is the flux density (luminosity per Hertz, $\text{erg s}^{-1} \text{ Hz}^{-1}$), at frequency ν .

The Lyman edge luminosity $L_0 \sim \nu_0 L_{\nu_0}$ is not known for ULIRGs, but it is likely to be much less than the flux at longer wavelengths, for two reasons. First, most ULIRGs are powered primarily by stars, which have large intrinsic Lyman edges. ULIRGs powered by AGN may have larger Lyman luminosities; if so they should show less absorption in NaI. Second, the dusty gas both in the galaxy proper and in the outflows will have a substantial (perhaps dominant) fraction of neutral hydrogen, which will absorb radiation beyond the Lyman edge. With our canonical values for mass loss rate (and hence density), and for expected Lyman edge fluxes ($L_0 \lesssim 10^{42} \text{ erg s}^{-1}$, corresponding to smooth extrapolations from UV flux density ratios $L_{\nu}^0 / L_{\nu}^{FIR} \approx 10^{-6}$, see Figure 2), the neutral fraction of hydrogen is at least 10^{-4} ; the column through the ULIRG wind is of order 10^{21} cm^{-2} , so the wind has an optical depth of order unity at the edge.

Galaxies with no intrinsic Lyman edge and large UV to FIR flux density ratios

$$L_{\nu}^{UV} / L_{\nu}^{FIR} > 10^{-5} \quad (26)$$

will then have ionized winds, independent of any possible heating due to shocks or supernova driving. Such winds will not contain an observable column of neutral sodium.

In contrast, galaxies that have no intrinsic Lyman edge but which have flux density ratios less than 10^{-5} will have

winds that are optically thick at the edge, as will almost any galaxy with an intrinsic Lyman edge. In such galaxies the wind will consist primarily of (nearly) neutral hydrogen, assuming that it is not strongly heated by supernovae or an AGN. Such galaxies may or may not have substantial columns of neutral sodium, as we now show.

In gas in which hydrogen is nearly neutral, the neutral fraction of sodium is given roughly by

$$\frac{n_{\text{NaI}}}{n_{\text{NaII}}} \approx \frac{\alpha_{\text{NaI}}}{\alpha_{\text{NaI}} c} \frac{n_e}{n} U_{\text{NaI}}^{-1}, \quad (27)$$

where

$$U_{\text{NaI}} \equiv \frac{L_{\text{NaI}} / \langle h\nu_{ed} \rangle}{4\pi r^2 n c} \quad (28)$$

is the ratio of the number density of NaI ionizing photons to the number density of hydrogen. The subscript *ed* refers to the sodium photoionization edge, i.e.. $\lambda_{ed} \approx 0.2\mu\text{m}$, and the quantity in angular brackets is the average energy of ionizing photons. The numerator in this definition is, by analogy with equation (25)

$$\frac{a_{\nu_{ed}, \text{NaI}} L_{\text{NaI}}}{\langle h\nu_{ed} \rangle} \equiv \int_{\nu_{ed}}^{\infty} d\nu \frac{a_{\nu, \text{NaI}} L_{\nu}}{h\nu}. \quad (29)$$

Combining these expressions, we estimate the neutral fraction of Na as

$$\frac{n_{\text{NaI}}}{n_{\text{NaII}}} = \frac{\alpha_{\text{NaI}}}{a_{\nu_{ed}, \text{NaI}}} \frac{4\pi r^2 n_e \langle h\nu_{ed} \rangle}{L_{\text{FIR}}} \frac{\lambda_{ed}}{\lambda_{\text{FIR}}} \frac{L_{\nu}^{\text{FIR}}}{L_{\nu}^{\text{UV}}} e^{\tau_d}, \quad (30)$$

The factor e^{τ_d} accounts for the possible presence of dust. We remarked above that the lack of NaD emission lines together with the correlation of NaD absorption with reddening suggests that the outflows are dusty, but, as also noted above, the outflows do not cover the galaxy. The light that we see is thus a mixture of starlight directly from the galaxy combined with light filtered through the dusty wind. The sodium ions, on the other hand, are embedded in the wind, so they see the starlight after it has been filtered through the dust in the wind interior to their position. To account for this, the flux L_{ν}^{UV} should be reduced from that observed by a factor $\sim e^{-\tau_d}$, where τ_d is some appropriate fraction of the dust optical depth through the wind. The hydrogen column through the wind is uncertain (since the conversion from Na to H columns is uncertain), but if the mass loss rate is of order the star formation rate the hydrogen column is of order $5 \times 10^{21} \text{ cm}^{-2}$ (see equation 3). Assuming a galactic gas to dust ratio, the dust optical depth would be $\tau_d \sim 2$ in the UV. Numerically,

$$\frac{n_{\text{NaI}}}{n_{\text{NaII}}} \approx 4 \times 10^{-9} \frac{L_{\nu}^{\text{FIR}}}{L_{\nu}^{\text{UV}}} \left(\frac{n}{1 \text{ cm}^{-3}} \right), \quad (31)$$

where we have taken $\tau_d = 1$. In terms of U_{NaI} ,

$$\frac{n_{\text{NaI}}}{n_{\text{NaII}}} \approx 3 \times 10^{-4} / U_{\text{NaI}}. \quad (32)$$

This expression is valid for $U_{\text{NaI}} \gtrsim 10^{-3}$. For values of the ionization parameter less than this, the neutral sodium fraction will saturate (at a value of order 0.5, see the numerical results below).

We will see that if the cool outflow is driven by a hot wind with a mass loss rate comparable to the star formation rate, and the cool component has a similar mass loss rate, U_{NaI} ranges from 10^{-7} to 10^{-3} ; for a dust driven outflow with the same mass loss rate the range is $10^{-3} \lesssim U_{\text{NaI}} \lesssim 10$.

The object to object variation in the UV flux is most naturally explained by variations in the dust optical depth along our line of sight; thus it may be appropriate to set τ_d to some smaller value in objects with (relatively) large UV fluxes. On the other hand it is possible that even in objects with large UV fluxes the hydrogen column through the wind is still of order 10^{21} cm^{-2} , but that some of the star formation is unobscured; even in the object with the highest UV flux in the Goldader et al. (2002) sample, the UV flux is less than a tenth of the bolometric flux. The mass loss rate may or may not be affected by this bolometrically small UV flux. If it is not, then $\tau_d \approx 1$ would be appropriate even for those objects with large UV fluxes.

We were not able to find photometry in the UV bands for the IRAS sources in Martin (2005) or in Rupke et al. (2005a). As a proxy, we used the SEDs for the luminous infrared galaxies observed by Goldader et al. (2002). The data, obtained from NED, are shown in Figure 2. The flux density near the Na I edge (about 0.2 microns) is smaller, relative to the bolometric luminosity, in Arp 220 than in IRAS 15250+3609. The difference is roughly a factor of 90; The relative Na I edge flux density in VV 114 is another factor of 4 larger than that in IRAS 15250+3609. The other objects in Goldader et al. (2002), IRAS 08572+3915, Mrk 273, IC 883, and IRAS 19245-7245, have flux ratios intermediate between IRAS 15250+3609 and Arp 220. We note that Mrk 273 is an AGN, with a luminosity between a Seyfert and a quasar. Despite this fact, it has a modest UV flux.

Since the Na edge flux densities of our proxy galaxies differ by a factor of ~ 90 (for the same FIR flux) we expect a similar difference in the fraction of neutral Na in their outflows. For VV 114, with $L_{\nu}^{\text{UV}} / L_{\nu}^{\text{FIR}} \approx 10^{-4}$, equation (30) predicts a neutral fraction of $\sim 2 \times 10^{-5} (n/1 \text{ cm}^{-3}) e^{\tau_d}$; for Arp 220, with $L_{\nu}^{\text{UV}} / L_{\nu}^{\text{FIR}} \approx 2 \times 10^{-7}$, the predicted neutral fraction is $\sim 0.01 (n/1 \text{ cm}^{-3}) e^{\tau_d}$.

3. NUMERICAL CALCULATIONS

We have carried out numerical calculations of the photoionization state of gas irradiated by sample ULIRG spectral energy distributions (SED). These calculations were performed with version 06.02.09a of Cloudy, last described by Ferland et al. (1998). For the sake of simplicity we modeled the wind using a constant density slab, with six different densities (6, 60, 600, 6000, 6×10^4 and $6 \times 10^5 \text{ cm}^{-3}$), with the lowest and highest densities corresponding to a smooth cold outflow and to a clumpy cold medium in pressure equilibrium in a hot outflow with mass loss rate equal to the star formation rate. The intermediate densities model clumpy cold outflows not driven by hot gas. Dust grains were included in the model; we used the ISM option of cloudy, which depletes the gas abundances so that the total metallicity, gas plus dust, is solar. The

dust and gas are mixed in the slab, which lies between the continuum source and the observer.

For each density the cold gas is illuminated by various SEDs, all having a total luminosity of $10^{12}L_{\odot}$, appropriate for ULIRGs. Three of the SEDs employed were those of VV 114, IRAS 15250+3609, and Arp 220. In addition we calculated a series of models based on the SED of Arp 220. In these models we adjusted the flux density at 5.1eV ($\approx 2400 \text{ \AA}$), varying the FIR to UV ratio from $L_{\nu}^{UV}/L_{\nu}^{FIR} = 10^{-9}$ to 10^{-4} . In doing so we fit a power law from the last IR data point to 2400 \AA . From 2400 to 1450 \AA we assumed that νL_{ν} was flat, i.e., $L_{\nu} \sim \nu^{-1}$ as in the 2kpc data of Goldader et al. (2002) for Arp 220. From 1450 \AA to the Lyman edge we simply continued the spectrum with the same slope, $L_{\nu} \sim \nu^{-1}$.

We note that the UV slope for many of the galaxies in Goldader et al. (2002) varies with the aperture size, and that the total flux scales roughly with the square of the aperture size, the latter indicating that the UV flux emerges from a much larger region than the radio or CO emission. If the same holds true for the ULIRGs in general, the UV flux will not decrease as rapidly with distance from the galactic center as will the density in a smooth outflow. The result will be an increasing ionization parameter with increasing radius; if the cool gas is clumpy, and not pressure confined, then the density will not decrease as $1/r^2$, and the ionization parameter will not increase as rapidly as in a smooth wind. We have not attempted to model such effects.

For models with no intrinsic Lyman edge, the spectrum from 13.6 eV to the lone x-ray point at 1 KeV was a simple power law. In models with an intrinsic Lyman edge, the spectrum from the edge to the x-ray point was also a power law, but with a discontinuity at the energy corresponding to the Lyman edge.

We explored other SEDs. We found that the details of the continuum shortward of 2400 \AA do not matter as long as the Lyman edge flux is small enough; if the fraction of neutral hydrogen is larger than about 10^{-4} ($U < 10^{-2}$) at the face of the slab, the wind is optically thick at the Lyman edge and the NaI fraction is controlled by the flux at the NaI edge. If this condition on the neutral hydrogen fraction is not met, there is essentially no neutral sodium unless an unphysically large column ($N_H > 10^{22} \text{ cm}^{-2}$), sufficient to produce a Lyman edge, is used.

Calculations with CLOUDY verify the simple arguments made in the previous section; the neutral fraction of Na can vary by factors of 100 or more due to variations in the SED of the host galaxy. The neutral fraction varies from a maximum near 1 for an SED with a UV to FIR flux density ratio of 10^{-8} to a low of 10^{-4} for the spectrum of VV 114 (assuming a substantial Lyman break; if there is no break, the neutral fraction of Na can be much smaller).

Figure 3 shows the input spectrum of a CLOUDY run, the spectrum transmitted through the outflow, and the sum of the transmitted and emitted spectrum. The UV to FIR flux density ratio is 10^{-7} at the face of the slab, and there is no Lyman edge. After passing through the slab, the spectrum exhibits a strong Lyman edge, and strong resonance lines, including Lyman alpha. The effect of dust

attenuation can be also seen clearly; this attenuation enhances the fraction of Na I over what is seen in calculations with no dust. The dashed lines show a similar calculation in which an intrinsic Lyman edge appears in the input spectrum (which has been shifted downward to distinguish the two cases). Note the lack of prominent emission lines, since there are few ionizing photons to power such emission.

Figure 4 shows the ratio N_{NaI}/N_{Na} as a function of the UV (evaluated at 2000 \AA) to FIR (100 micron) flux density ratio for a range of densities. We have assumed that the flux shortward of the Lyman edge is a factor of 10 lower than on the long wavelength side. From the last UV data point to the edge we assumed a power law of the form $L_{\nu} \sim \nu^{-1}$; from just shortward of the edge to the first x-ray data point we assumed a simple power law.

The open points correspond to the artificial SEDs based on the SED of Arp 220, assuming a Lyman edge. The density is held constant at the value $n = 6 \text{ cm}^{-3}$ (open triangles), $n = 60 \text{ cm}^{-3}$ (squares), 600 cm^{-3} (pentagons), 6000 cm^{-3} (hexagons), $6 \times 10^4 \text{ cm}^{-3}$ (circles), and $6 \times 10^5 \text{ cm}^{-3}$ (filled squares); the open triangles corresponds to a completely smooth wind with $\dot{M}_w = 22M_{\odot}/\text{yr}$, the filled squares to pressure confined cold clouds in hot gas with a mass loss rate equal to the star formation rate.

The crosses correspond to the artificial Arp 220 SEDs, assuming no Lyman edge, and a smooth wind. The lower neutral sodium column in the no-edge case compared to the intrinsic-edge case arises as follows: Lyman continuum photons penetrating the inner face of the slab keep hydrogen ionized until the optical depth at the Lyman edge reaches unity; beyond that depth hydrogen recombines, and the neutral fraction of sodium is essentially the same as in the case of an SED with an intrinsic Lyman edge. When the ‘‘Stromgren depth’’ is larger than the column in the wind, as when the UV/FIR ratio is 10^{-4} , the neutral fraction of sodium is tiny ($\sim 10^{-9}$), so the corresponding cross in Figure 4 is off the bottom of the plot.

The dashed line in Figure 4 gives the prediction of equation (30), which agrees well with the more complete calculation for UV/FIR ratios larger than $\sim 10^{-7}$, in the case of an intrinsic Lyman edge.

The three filled triangles correspond to the measured values of NaI for Arp 220, Mrk 273 (data for both taken from Heckman et al. 2000), and IRAS 23365+3604 (NaI column from Martin 2005), as labeled in the figure. In each case we assumed that the mass loss rate from the host galaxy was given by equation (6), then use the observed NaI column to find the ionization fraction. The error bars reflect only the variation in η found by Rupke et al (2005b), i.e., only the apparent variation in the mass loss rate for objects of the same luminosity. To estimate the (unknown) flux at the NaI edge for IRAS 23365+3604 we extrapolated from the nuclear (2.5 kpc) U-band measurement of Surace & Sanders (2002), assuming a power law extending from the last two optical data points. This extrapolation is highly uncertain, as a glance at Figure 2 shows.

With only three data points, those corresponding to Arp 220, Mrk 273, and IRAS 23365, the interpretation of Fig.

4 is uncertain. In particular, there is no clear trend of Na column with UV flux. The three data points correspond to densities in the range $60 - 6000 \text{ cm}^{-3}$, suggesting that the flow is slightly clumpy, but not in pressure equilibrium with a hot flow of the same total mass loss rate. Clearly more measurements of near UV fluxes for galaxies in either or both the Rupke et al. and Martin samples are called for.

Figure 5 is similar to Figure 4, except that the ion fraction plotted is that for Magnesium II over the total Magnesium abundance. The bulk of the magnesium is singly ionized for $n < 6 \times 10^4 \text{ cm}^{-2}$; even for higher densities most of the atoms are singly ionized for UV to FIR flux density ratios larger than 10^{-5} . The near-UV resonance transition of MgII should be a good tracer of neutral outflows; if the MgII column is seen to anti-correlate with UV flux, while the NaI column does not vary with UV, it would suggest that the cool gas has a high density and is therefore probably driven out by hot gas. If the MgII column does not vary with UV flux, while the NaI column does, then the gas is most likely low density, and not driven out of the galaxy by hot gas.

4. DISCUSSION

We have identified two plausible sources of variation in the ionization fraction of NaI toward ULIRGs, variations in the (NaI) ionizing radiation, and global object-to-object variations in gas density. The limited observations of UV fluxes from ULIRGs (essentially the objects in Goldader et al. 2002) suggest that the former source of variation may well be happening.

Variations in the globally averaged density of outflowing gas translate into variations in filling factor of dense gas if we assume that \dot{M}_w does not vary much from object to object. The filling factor might vary, if, for example, the cold gas were in pressure equilibrium with hot gas, but the mass loss rate of hot gas varied from ULIRG to ULIRG. Another possible source of variation in filling factor might be global differences in the outflow, leading to stronger or weaker shocks and hence higher or lower post-shock densities. However, because the sound crossing times of the clumps are smaller than the outflow time, this source of variation does not appear to us to be very promising—the clumps would simply re-expand until they reach pressure equilibrium.

Another possible source of variation is variable depletion onto dust grains. If high velocity shocks pass through the gas they will destroy the dust grains, so that no Na is depleted onto dust. As we have indicated above, there is observational evidence that dust survives in the outflows, so perhaps any shocks that have passed through the gas are not strong. On the other hand, if the hot gas has a high pressure, the density of the cold gas may well be high enough to regrow grains, or to cause further depletion of Na onto any grains that survive. We have not attempted to work out the physics of these processes.

The referee kindly pointed out that observations of NGC 6240 Veilleux et al. (2003) show emission lines consistent with shock ionization. As we noted above, the column of the shock-illuminated and -ionized gas is small compared

to the total column in the outflow. The emission lines may be dominated by shock ionization, but it does not follow that the bulk of the gas in the wind is. A clear way to tell the difference between photoionized and shock-ionized flows is to look for a systematic variation of NaI columns with UV flux. If such a correlation is found, the gas is photoionized. If there is no such correlation, then it is shock ionized. (The scaling of UV flux with aperture size found by Goldader et al. 2002 shows that in their galaxies at least, the UV emission is not dominated by that produced in shocks in a wind).

5. CONCLUSIONS

The mass loss rates of ultraluminous infrared galaxies, as determined by observations of the NaD lines, are believed to be substantial—of order one fifth of the star formation rate. This estimate assumes that the ionization fraction of sodium is ~ 0.1 . The gross physical properties of ULIRGs, including their stellar masses, gas masses, sizes, and star formation rates vary by factors of only a few, so at first glance the assumption of fixed NaI ionization fraction appears reasonable. However, one property of ULIRGS that appears, based only on a few galaxies, to vary by a large amount is the ultraviolet flux. We have shown that cool ULIRG winds are likely to be in photoionization equilibrium. We used a simple argument to show that the large object-to-object UV flux variations seen in the small number of galaxies that have been observed in the ultraviolet would be enough to produce similarly large variations in NaI column density, if the density of the cool gas is $n \lesssim 10^5 (500 \text{ pc}/r)^2 \text{ cm}^{-3}$. More complete photoionization calculations using CLOUDY produce the same magnitude of variation in NaI/Na with variation in UV flux. They also show, for these moderate densities, that the MgII column should not vary appreciably with changes in UV flux.

If, however, the cold gas is in pressure equilibrium with a hot wind having a mass loss rate similar to the star formation rate of a typical ULIRG, the cool gas will have a density $n \gtrsim 10^6 (500 \text{ pc}/r)^2 \text{ cm}^{-3}$. In that case the ionization parameter is $U_{\text{NaI}} < 10^{-3}$, and there will be little variation in NaI column from object to object. As a check, the (so far unobserved) MgII columns are predicted to show variations that are anti-correlated with the UV/FIR ratio.

We conclude that the observed factor of ~ 100 variation in the UV/FIR flux density ratios in ULIRGs with similar bolometric luminosities is consistent with the factor of ~ 40 variations in the column density of Na I outflows seen by Martin (2006) and Rupke et al. (2005a); the different UV fluxes may well be the cause of the variation seen in the NaI columns, if the cool gas has a density $n \lesssim 10^5 \text{ cm}^{-3}$. A tight correlation between Na I column and UV flux would indicate that the cool gas is not accelerated by a hot wind.

The origin of the object-to-object variation in the UV/FIR ratio is not clear. The known correlation between reddening and NaI column in lower luminosity galaxies suggests that dust in the outflow may play a role. However, the NaI optical depth toward luminous infrared galaxies in the sample of Rupke et al. (2005b) actually exceeds that toward their (more luminous) ULIRGs. It is unlikely that the UV/FIR ratio is smaller in the less luminous objects.

Thus dust absorption in the outflow is probably not the sole reason for the low UV fluxes in ULIRGS.

Whether the galaxies studied by Martin (2005) and by Rupke et al. (2005a,2005b) actually have large object-to-object variations in their near-UV fluxes is not known. We note that the results of Goldader et al. (2002) show that near IR or even optical flux measurements are not a good proxy for the UV flux; see the data for VV114, IRAS 15250+3609, and Mrk 273 in Figure 2. This demonstrates that optical observations will not be sufficient to answer this question. Observations by GALEX or by the ACS on the Hubble Space Telescope could answer this question

definitively.

N.M. is supported in part by the Canada Research Chair program and by NSERC. E.Q. is supported in part by NSF grant AST 0206006, NASA grant NAG5-12043. Both E.Q. and C. M. were supported by grants from the Alfred P. Sloan Foundation, and the David and Lucile Packard Foundation. This research has made use of the NASA/IPAC Extragalactic Database (NED) which is operated by the Jet Propulsion Laboratory, California Institute of Technology, under contract with the National Aeronautics and Space Administration.

REFERENCES

- Anders, E., & Grevesse, N. 1989, *Geochim. Cosmochim. Acta*, 53, 197
- Dalgarno, A., & McCray, R. A. 1972, *ARA&A*, 10, 375
- Clements, D. L., McDowell, J. C., Shaked, S., Baker, A. C., Borne, K., Colina, L., Lamb, S. A., & Mundell, C. 2002, *ApJ*, 581, 974
- Condon, J. J., Huang, Z.-P., Yin, Q. F., & Thuan, T. X. 1991, *ApJ*, 378, 65
- Ferland, G. J., Korista, K. T., Verner, D. A., Ferguson, J. W., Kingdon, J. B., & Verner, E. M. 1998, *PASP*, 110, 761
- Goldader, J. D., Meurer, G., Heckman, T. M., Seibert, M., Sanders, D. B., Calzetti, D., & Steidel, C. C. 2002, *ApJ*, 568, 651
- Heckman, T. M., Lehnert, M. D., Strickland, D. K., & Armus, L. 2000, *ApJS*, 129, 493
- Martin, C. L. 1999, *ApJ*, 513, 156
- Martin, C. L. 2005, *ApJ*, 621, 227
- Martin, C. L. 2006, *ArXiv Astrophysics e-prints*, arXiv:astro-ph/0604173
- McClure-Griffiths, N. M., Ford, A., Pisano, D. J., Gibson, B. K., Staveley-Smith, L., Calabretta, M. R., Dedes, L., & Kalberla, P. M. W. 2005, *ArXiv Astrophysics e-prints*, arXiv:astro-ph/0510304
- McDowell, J. C., et al. 2003, *ApJ*, 591, 154
- McKee, C. F., & Hollenbach, D. J. 1980, *ARA&A*, 18, 219
- Murray, N., Quataert, E., & Thompson, T. A. 2005, *ApJ*, 618, 569
- Osterbrock, D. E. 1989, *Astrophysics of Gaseous Nebulae and Active Galactic Nuclei* (Mill Valley, CA: University Science Books)
- Rupke, D. S., & Veilleux, S. 2005, *ApJ*, 631, L37
- Rupke, D. S., Veilleux, S., & Sanders, D. B. 2002, *ApJ*, 570, 588
- Rupke, D. S., Veilleux, S., & Sanders, D. B. 2005a, *ApJS*, 160, 87
- Rupke, D. S., Veilleux, S., & Sanders, D. B. 2005b, *ApJS*, 160, 115
- Sakamoto, K., Scoville, N. Z., Yun, M. S., Crosas, M., Genzel, R., & Tacconi, L. J. 1999, *ApJ*, 514, 68
- Savage, B. D., & Sembach, K. R. 1996, *ARA&A*, 34, 279
- Solomon, P. M., Downes, D., Radford, S. J. E., & Barrett, J. W. 1997, *ApJ*, 478, 144
- Surace, J. A., & Sanders, D. B. 2000, *AJ*, 120, 604
- Sutherland, R. S., & Dopita, M. A. 1993, *ApJS*, 88, 253
- Veilleux, S., Kim, D.-C., Sanders, D. B., Mazzarella, J. M., & Soifer, B. T. 1995, *ApJS*, 98, 171
- Veilleux, S., Shopbell, P. L., Rupke, D. S., Bland-Hawthorn, J., & Cecil, G. 2003, *AJ*, 126, 2185
- Verner, D. A., & Ferland, G. J. 1996, *ApJS*, 103, 467
- Verner, D. A., Ferland, G. J., Korista, K. T., & Yakovlev, D. G. 1996, *ApJ*, 465, 487

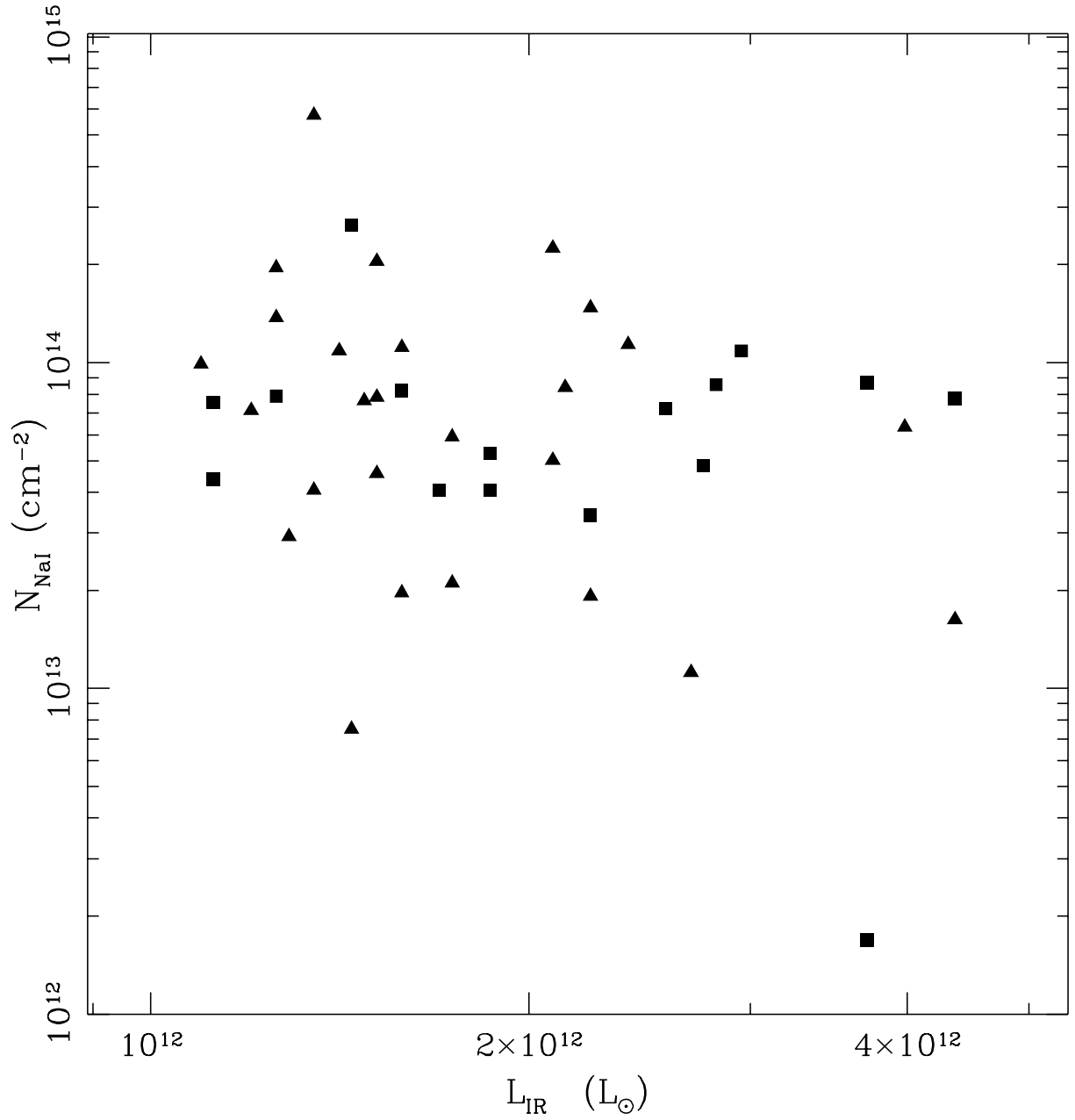


FIG. 1.— Neutral sodium (NaI) column as a function of galactic infrared luminosity. Data taken from Rupke et al. (2005a) (triangles) and Martin (2006) (squares). The Martin results are for sightlines toward the respective galactic centers. Note the large spread in the column for galaxies of approximately the same infrared luminosity.

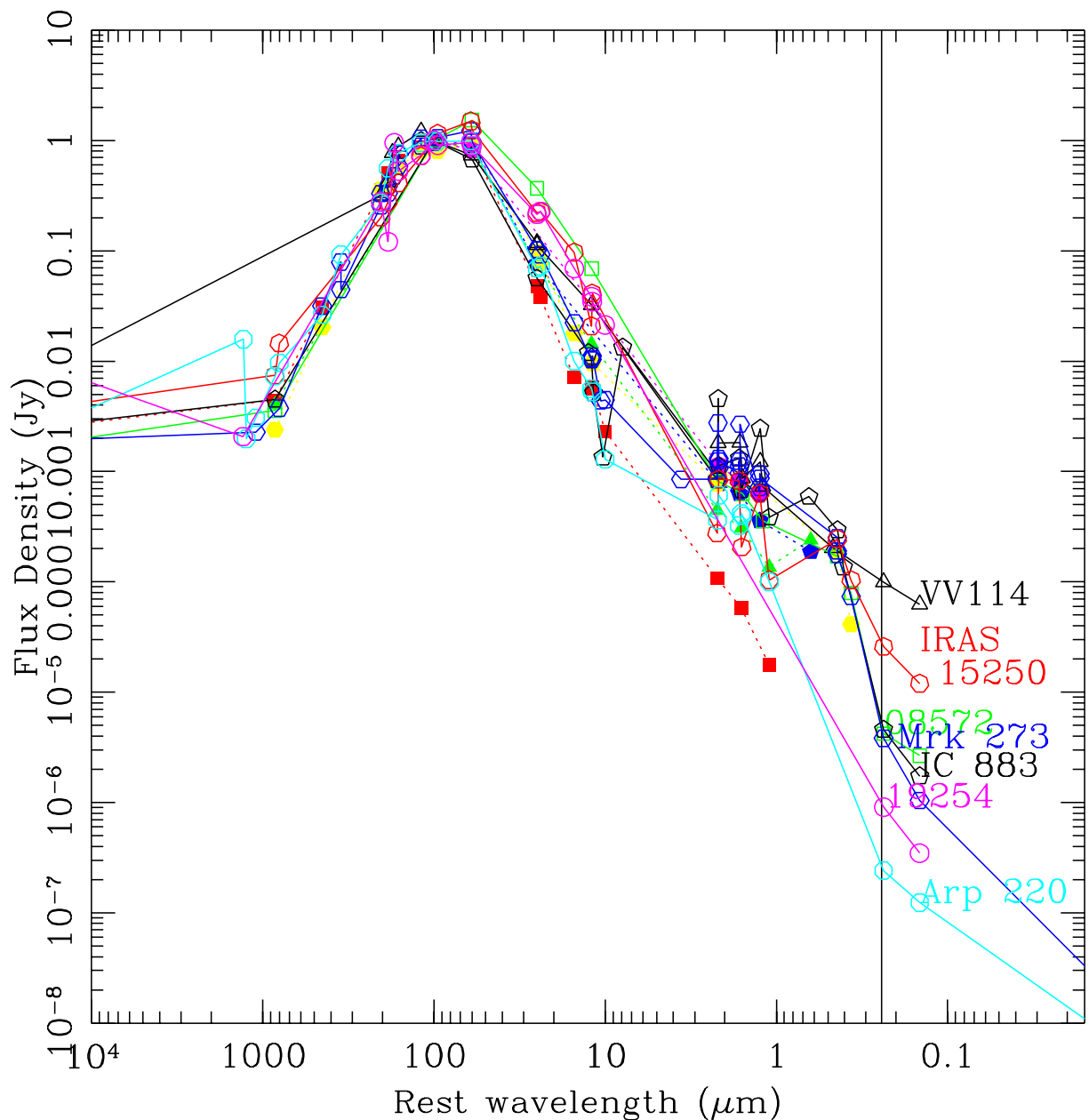


FIG. 2.— Spectral energy distributions of various ULIRGs, normalized to unity at $100\mu\text{m}$; data from the NASA/IPAC Extragalactic Database (NED), supplemented by Goldader et al. (2002) (we plot the 2kpc aperture data) and Martin (2005). The solid symbols represent objects from Martin (2005); triangles, IRAS 10565+2448; squares, IRAS 17208-0014; pentagons, IRAS 19297-0406; hexagons, IRAS 23365+3604; septagons, IRAS 00153+5454. The open symbols are from objects with HST UV observations by Goldader et al. (2002); triangles, VV 114; squares, IRAS 08572+3915; pentagons, IC 883; hexagons, Mrk 273; septagons, IRAS 15250+3609; octagons, Arp 220; and circles, IRAS 19254-7245. The UV/FIR flux density ratio varies by a factor of ~ 100 between Arp 220 and IRAS 15250+3609, and by ~ 300 from Arp 220 to VV 114. The vertical solid line is at the wavelength of the NaI ionization edge.

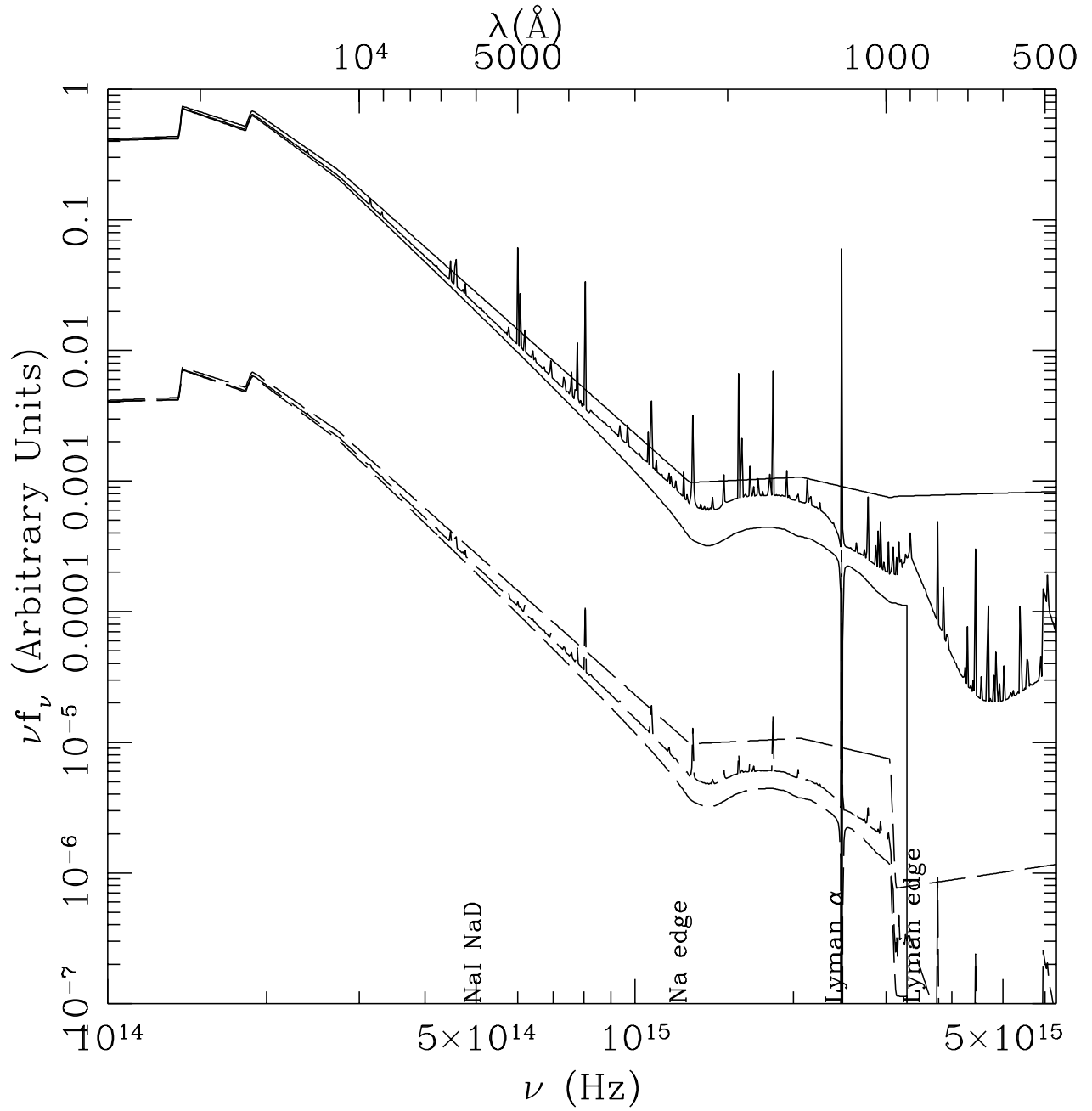


FIG. 3.— Input spectra of a CLOUDY model with a UV to FIR flux density ratio of 10^{-7} and no Lyman break (top solid lines) and with a Lyman break (top dashed curve); the latter has been displaced downward by a factor of one hundred to clarify the presentation. In both cases the middle curve shows the transmitted plus emitted spectrum, while the bottom curve shows the transmitted spectrum alone.

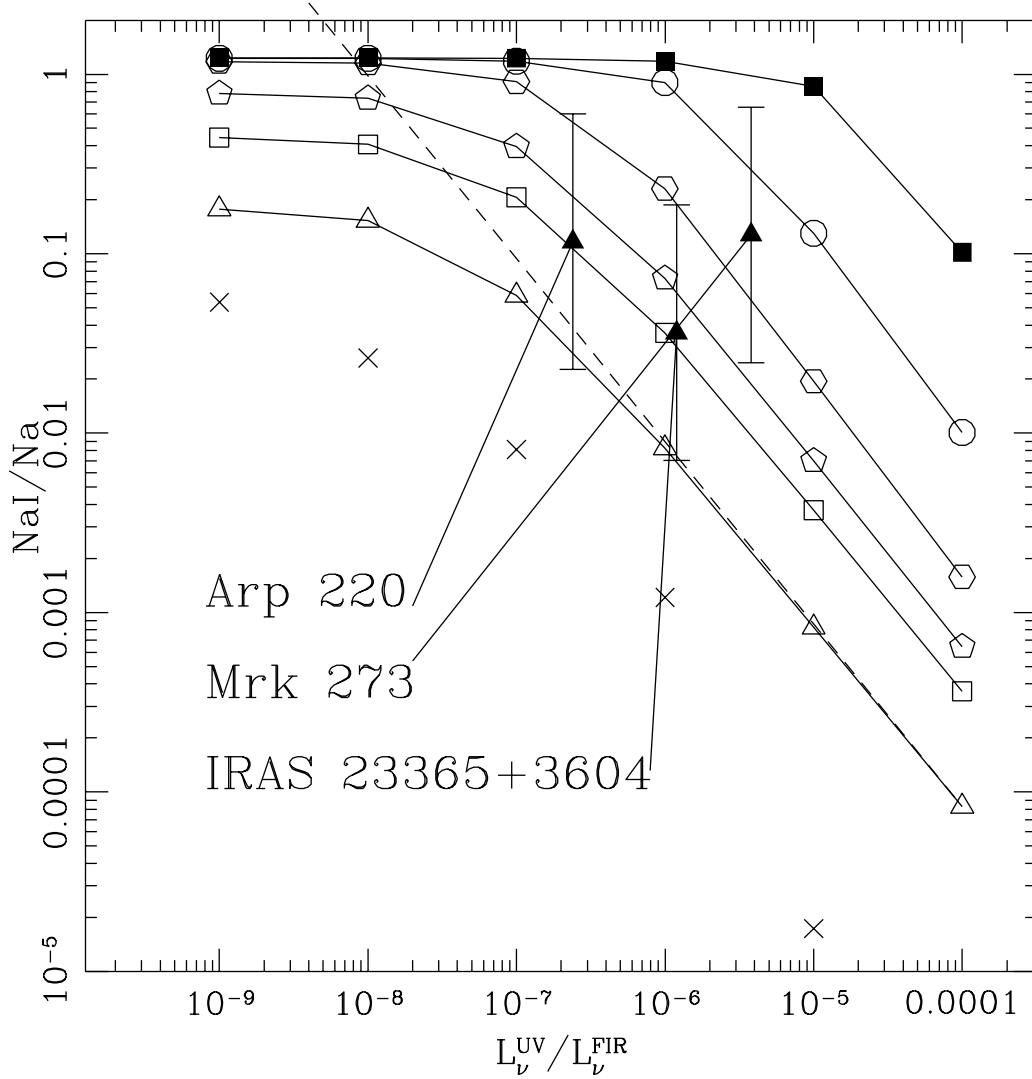


FIG. 4.— Neutral sodium fraction, N_{NaI}/N_{Na} , as a function of $L_{\nu}^{UV}/L_{\nu}^{FIR}$. The open polygons are calculated using the SED of Arp 220, but with the near UV data points altered to give various ratios of L_{UV}/L_{FIR} . The (assumed constant) density of the absorbing gas is $n = 6 \text{ cm}^{-3}$ (open triangles), corresponding to a smooth wind with $\dot{M}_w = 22M_{\odot}/\text{yr}$ at a distance $r_0 = 500 \text{ pc}$ from the source, $n = 60 \text{ cm}^{-3}$ (open squares), $n = 600 \text{ cm}^{-3}$ (pentagons), $n = 6000 \text{ cm}^{-3}$ (hexagons), and $n = 6 \times 10^4 \text{ cm}^{-3}$ (circles). The filled squares give the ionization fraction for $n = 6 \times 10^5 \text{ cm}^{-3}$, corresponding to cold gas in pressure equilibrium with a hot outflow with a mass loss rate equal to the star formation rate. The crosses correspond to $n = 6 \text{ cm}^{-3}$ and various flux density ratios, using SEDs with no Lyman edge. The dashed line is the prediction of equations (3) and (31) for $n = 6 \text{ cm}^{-3}$ for an SED with a Lyman edge. The solid points correspond to the measured NaI column for Arp 220, Mrk 274, and IRAS 23365+3604, under the assumption that $\dot{M}_w = \eta \dot{M}_{\odot}$, with $\eta = 0.25$, and $r_0 = 500 \text{ pc}$.

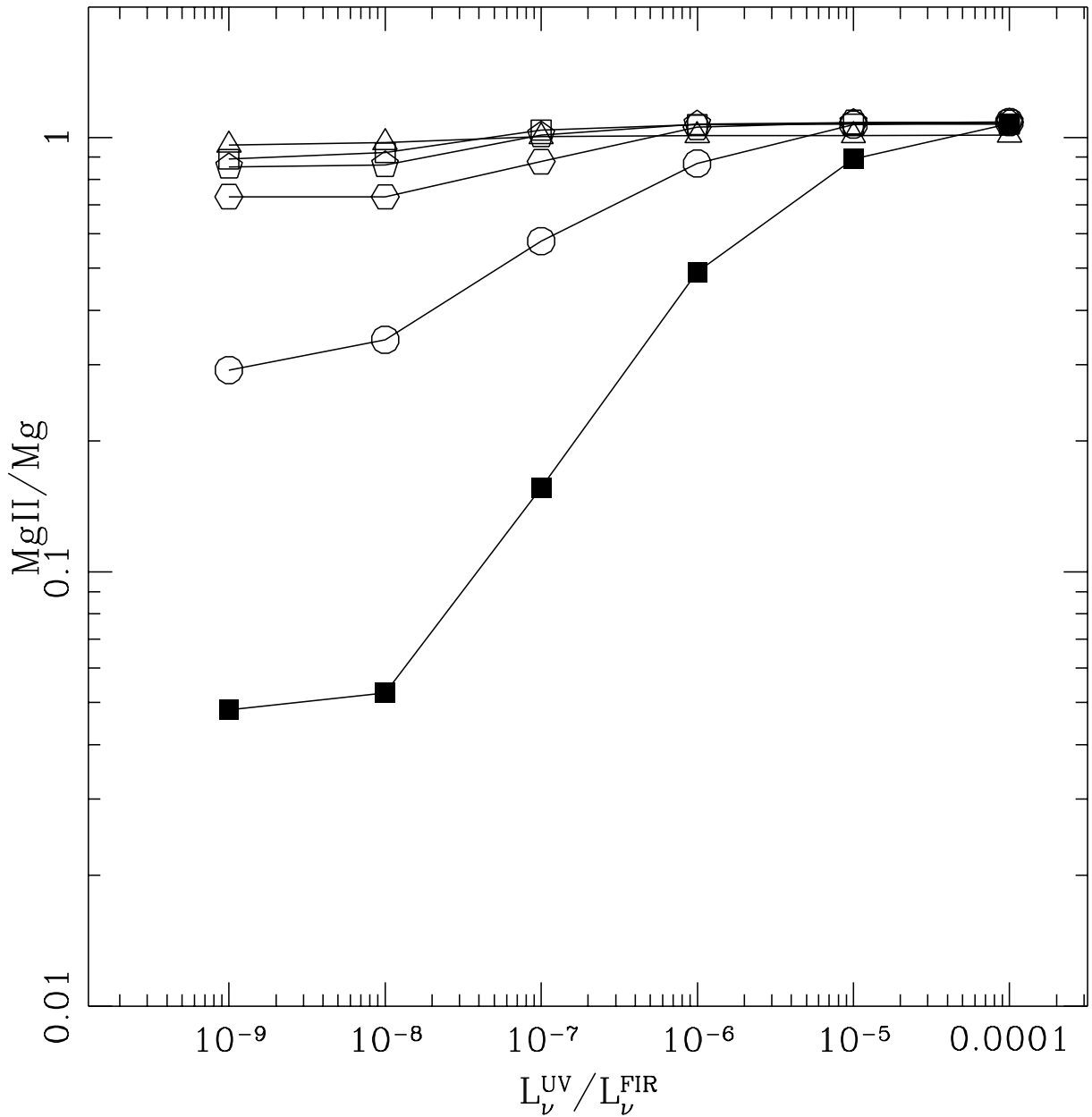


FIG. 5.— The ratio of Magnesium II to total Magnesium, N_{MgII}/N_{Mg} , as a function of $L_{\nu}^{UV}/L_{\nu}^{FIR}$. The SED's and symbols are as in Fig. 4. The bulk of the magnesium is singly ionized for all but the highest densities plotted. The column of MgII toward a ULIRG would be a *decreasing* function of L_{UV}/L_{FIR} , particularly for pressure confined high density clouds. This behavior is the opposite of that predicted for the NaI/Na ratio for similarly high density gas.